Simulation-Based Engineering Lab
University of Wisconsin-Madison

Technical Report TR-2016-17

Using the Complementarity and Penalty Methods for Solving Frictional Contact Problems in Chrono: Validation for the Standard Triaxial Test

Michał Kwarta and Dan Negrut

Version: January 25, 2017

Abstract

The numerical results of standard triaxial test were presented and validated against experimental ones. Two different approaches for modeling the dynamics of granular matter were used. The first one, discrete element method with penalty contact modeling (DEM-P) [1], is approach used in e. g. granular flows or powder mechanics simulations. The second method, called DEM-C (from "complementarity") is essential in fields like robotics and graphics [2]. In this approach the bodies cannot penetrate due to the complementarity conditions. Even though the methods use two very different approaches to model the contact with friction, as well as they can be described by using two different sets of mechanical and numerical parameters, the results obtained from the simulations were comparable. The validation study was enriched by the performance analysis. We also examined how sensitive the results are to the changes of certain parameters values. To obtain the results, an open source software package, called Chrono was used. The source code of the model used in the numerical experiments is also available on-line.

Keywords: standard triaxial test, penalty contact modeling, differential variational inequality modeling, friction, contact

Contents

Nomenclature

Abbreviations

DEM-P	Discrete Element Method - Penalty
DEM-C	Discrete Element Method - Complementarity
STT	Standard Triaxial Test

Physical parameters

Y	Young's modulus
ν	Poisson's ratio
ϱ	density
p	confining pressure
$\dot{\varepsilon}$	axial strain rate
$\mu_{\text{p-p}}$	inter-sphere coefficient of friction
$\mu_{\text{p-s}}$	coefficient of friction between particles and container's side walls
$\mu_{\text{p-w}}$	coefficient of friction between particles and container's bottom and top walls
$c_{\text{r,p-p}}$	inter-sphere coefficient of restitution
$c_{\text{r,p-s}}$	coefficient of restitution between particles and container's side walls
$c_{\text{r,p-w}}$	coefficient of restitution between particles and container's bottom and top walls

Numerical parameters

Δt	time step
MNoI	maximum number of iterations
CRS	contact recovery speed

1 Laboratory Experiments

1.1 Overview

The description of the standard triaxial test (STT) can be found in [3]. In this section the details important from the simulation point of view were pointed out.

The experiments were conducted on in the cylindrical container with a diameter of 101 mm and a height of 203 mm. Two types of granular material were used: the first one (monodisperse case) consisted of spheres 5 mm in diameter; the other one (polydisperse case) was a mixture of evenly distributed spheres with a diameter of 4, 5 and 6 mm. Between 15382 and 15420 beads were used in the empirical tests.

The particles were made of Grade 25 Chrome Steel of the following mechanical parameters: density, $\varrho = 7800\ \frac{\text{kg}}{\text{m}^3}$, Young's modulus, $Y = 2 \cdot 10^{11}$ Pa, Poisson ratio, $\nu = 0.28$ (Table 1). The inter-sphere friction coefficient ($\mu_{\text{particle-particle}},\ \mu_{\text{p-p}}$) as well as the coefficient of friction between the beads, the top and the bottom walls ($\mu_{\text{particle-wall}},\ \mu_{\text{p-w}}$) were measured in [4] and [5], giving the values of 0.096 and 0.28, respectively (Table 2).

Table 1: The values of **particles**' mechanical parameters

	Material	$\varrho\left[\frac{\text{kg}}{\text{m}^3}\right]$	Y [Pa]	ν
Granular material	Grade 25 Chrome Steel	7800	$2 \cdot 10^{11}$	0.28

Table 2: The values of mechanical parameters describing **contacts**

	$\mu_{\text{p-p}}$	$\mu_{\text{p-w}}$
Contacts' parameters	0.096	0.28

The laboratory experiments consisted of two stages. The aim of the first one (settling stage) was preparing a settled and compressed specimen for the second one - standard triaxial test stage, see Figure 1. To compress the specimen, a confining pressure p equal to $8 \cdot 10^4$ Pa was applied to the walls of the container. When the compressed granular material was in its equilibrium state, a stress boundary condition on the top wall was replaced with an axial strain rate ($\dot{\varepsilon}$) boundary condition keeping the pressure on the side walls equal to $8 \cdot 10^4$ Pa. The axial strain rate was equal to $0.0083\ \frac{\%}{\text{s}}$ (Table 3).

Table 3: The values of the mechanical parameters describing the laboratory test

	p [Pa]	$\dot{\varepsilon}\ \left[\frac{\%}{\text{s}}\right]$
Lab test parameters	$8 \cdot 10^4$	0.0083

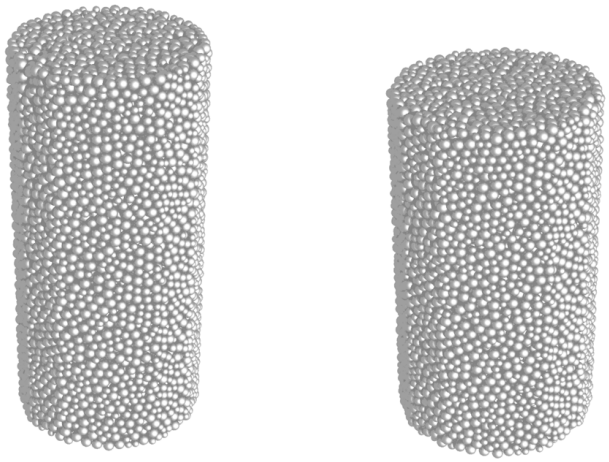

(a) (b)

Figure 1: Visualization of the numerical simulations of STT. Sample after the: (a) settling stage; (b) standard triaxial test stage.

1.2 Results

The void ratios of the settled samples were shown in Table 4. The *stress ratio - axial strain* curves obtained during the STT tests were presented in Figure 2. The stress ratio is defined as $(\sigma_1 - \sigma_3)/(\sigma_1 + \sigma_3)$, where:

σ_1 is the axial stress (the pressure that specimen acts on the **top wall** with) and

σ_3 is the pressure that specimen acts on the **side walls** with

The values of this stress ratio are related to the angle of the shearing resistance ϕ' by a following formula: $\sin(\phi') = (\sigma_1 - \sigma_3)/(\sigma_1 + \sigma_3)$. The angle of the shearing resistance is e. g. the angle between the side and the base of the cone formed of a granular material poured on the vertical surface [6].

Table 4: The range of the number of spheres used in the empirical tests and the void ratios obtained after the settling part

	Number of Spheres (Void Ratio)
Laboratory Experiments	1538 (0.615) ÷ 15420 (0.612)

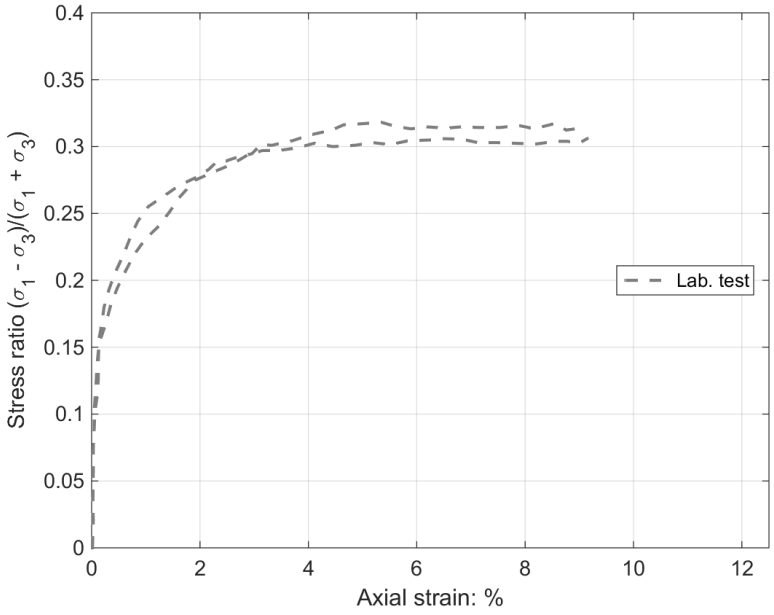

(a)

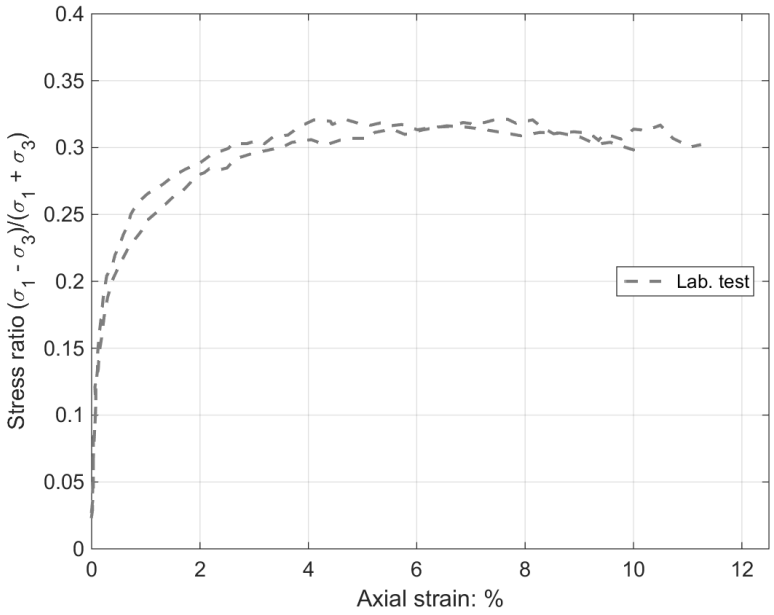

(b)

Figure 2: Experimental results. (a) Monodisperse specimen; (b) Polydisperse specimen.

2 Numerical Simulations

2.1 Physical Side of the Simulations

In the simulations, the following values were given to the mechanical parameters of particles: density, $\varrho = 7800\ \frac{\text{kg}}{\text{m}^3}$, Young's modulus, $Y = 2 \cdot 10^8$ Pa, Poisson ratio, $\nu = 0.28$. The walls of the container were treated as massless bodies and their mechanical parameters were given the same values (Table 5).

Table 5: The values of the **particles'** and **container's** mechanical parameters used in simulations

	$\varrho\left[\frac{\text{kg}}{\text{m}^3}\right]$	Y [Pa]	ν
Granular material	7800	$2 \cdot 10^8$	0.28
Container's walls	massless		

The inter-sphere friction coefficient and the coefficient of friction between the beads and the side walls ($\mu_{\text{particle-side}}, \mu_{\text{p-s}}$) were set to 0.096. The value of friction coefficient between the spheres and the top and bottom walls was equal to 0.28. The coefficient of restitution between particles and between the walls and particles were set to 0.597 [7] (Table 6).

Table 6: The values of the mechanical parameters describing **contacts** used in simulations

	$\mu_{\text{p-p}}$	$\mu_{\text{p-s}}$	$\mu_{\text{p-w}}$	$c_{\text{r,p-p}}$	$c_{\text{r,p-s}}$	$c_{\text{r,p-w}}$
Contacts' parameters	0.096	0.096	0.28	0.597	0.597	0.597

The axial strain rate used in the simulations was set to 10 $\frac{\%}{\text{s}}$. The reason for giving the axial strain rate value that is about 1000 times larger than it had been in the laboratory tests was to overcome the inconvenience of having a long simulation time. To neutralize the effects of compressing the specimen with a larger strain rate the material was made softer by setting the value of the beads' Young's modulus to 1000 times smaller number than it had been in reality. Confining pressure used in the numerical experiments was equal to $8 \cdot 10^4$ Pa.

	p [Pa]	$\dot{\varepsilon}\ \left[\frac{\%}{\text{s}}\right]$
STT's parameters	$8 \cdot 10^4$	10

Table 7: The values of mechanical parameters describing **STT** used in simulations

The simulations consisted of two stages: the settling stage and the standard triaxial test (STT) stage, see Figure 1. In the former one, after pouring the specimen into the container we applied the confining pressure, $p = 8 \cdot 10^4$ Pa, to its top and side walls and

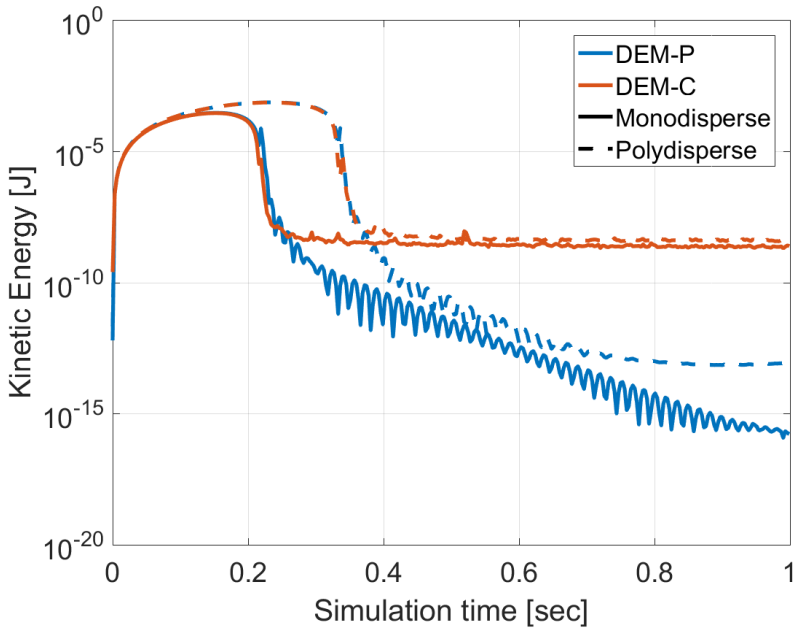

Figure 3: Evolution of system's kinetic energy during the settling stage of Standard Triaxial Test.

ran the simulation until the sample obtained its equilibrium state (Figure 3). Such prepared specimen was used in the latter stage, in which the confining pressure was kept on the side walls and the axial strain rate $\dot{\varepsilon}$ was applied to the top wall. The bottom wall in both stages was fixed.

2.2 Numerical Side of the Simulations

To simulate the standard triaxial test the mechanical system was modeled using two different methods of handling the friction and contact forces between colliding bodies: penalty (DEM-P) and complementarity (DEM-C) method. Those approaches can be successfully used in simulating the mechanical phenomena. If calibrated correctly, simulations based on DEM-P, as well as on DEM-C should give the results that are close enough to empirical measurements and also to each other. Correct calibration is equal to choosing the numerical values for the parameters the two approaches can be characterized with from the numerical point of view. Those values should provide stability of the computations and model the physics sufficiently well.

Stability of calculations in DEM-P model can be ensured by choosing the correct values of the time step (Δt). While using DEM-C method the combination of the following parameters: time step, contact recovery speed (CRS) and maximum number of iterations (MNoI) is important.

In both modeling approaches Δt is the parameter responsible for the stability of calcu-

lations. Too large value of the time step will make the simulations unstable, too small - will result in having very long execution time. The optimal value of Δt can be chosen using trial and error method. When it comes to the simulations run so far, the values of the time step used in the simulations based on the DEM-C usually were about 10 times larger than in DEM-P-based ones.

Contact recovery speed (CRS) is a parameter used only in DEM-C-based simulations. As its name indicates, it is a parameter that puts the upped limit on the normal component of the velocity two colliding bodies rebound off each other with. In complementarity approach the bodies are modeled as they were rigid. Even though, at the beginning of each time step bodies can overlap, assigning the penetration depth to such contact. In each time step, the normal component of the velocity two bodies will rebound off each other is equal to the penetration depth divided by the time step. If the value of this component exceeds the value of the upper limit (called contact recovery speed) it is simply clamped to the value of this limit. In other words, CRS provides stability to the simulations and allows having larger values of Δt and at the same time smaller amount of maximum number of iterations per time step (MNoI). Thus, it also makes the execution time of the simulations shorter.

MNoI sets the maximum number of iterations that are done during each time step to calculate the values of the normal and tangential components of forces related to every contact. The value of this parameter depends on the type of the simulations. In the simulation of cone penetration test (CPT) 50 iterations per time step were enough to have reasonable results [8]. Calculations with MNoI set up to 600 gave the satisfactory results concerning shear test [9]. The simulations of standard triaxial test required the value of MNoI to be set to 2500, to have calculation that were not only stable but also giving results correct from the physical point of view. The values of the above-described parameters used in the simulations of STT were presented in Table 8.

Table 8: Numerical parameters' values used in the simulations
* MNoI - maximum number of iterations
** CRS - contact recovery speed
*** if calculation in settling stage were done with CRS equal to $0.02\frac{\mathrm{m}}{\mathrm{s}}$, in standard triaxial test stage stability could be obtain for CRS set to larger values (even to $10^{30}\frac{\mathrm{m}}{\mathrm{s}}$)

		Monodisperse Sample		Polydisperse Sample	
Approach	Parameter	Settling	STT stage	Settling	STT stage
DEM-P	Δt [s]	$3 \cdot 10^{-5}$		$5 \cdot 10^{-5}$	
DEM-C	Δt [s]	10^{-4}		10^{-4}	
	MNoI**	700	2500	700	2000
	CRS* $[\frac{\mathrm{m}}{\mathrm{s}}]$	0.02	$0.02 \leq$***	0.02	$0.02 \leq$***

2.3 Results

In the laboratory tests between 15382 and 15420 spheres were used, giving the void ratios of 0.615 and 0.612, respectively. In the simulations to fill out the container we used 15918 spheres in the monodisperse and 15740 in the polydisperse case. The void ratios of simulated specimen in its equilibrium state ranged from 0.611 to 0.660, see Table 9.

Table 9: Comparison of number of spheres used and void ratios obtained after the settling part of the simulations and the laboratory experiments. Mono. - monodisperse case; Poly. - polydisperse case

		Spheres	Void Ratio (Relative Error Range [%])
Lab. Exp.		15382 ÷ 15420	0.615 ÷ 0.612
Mono.	DEM-P	15918	0.641 (4.06 ÷ 4.52)
	DEM-C		0.611 (0.65 ÷ 0.16)
Poly.	DEM-P	15740	0.660 (6.82 ÷ 7.27)
	DEM-C		0.626 (1.76 ÷ 2.24)

The comparison of the experimental and numerical results is illustrated in Fig. 4. The data obtained from our numerical computation was processed and compared to the plots of the variation in the stress ratio $(\sigma_1 - \sigma_3)/(\sigma_1 + \sigma_3)$ as a function of axial strain, published in the literature [10]. The numerical results matched the experimental ones with a fair precision. Additionally, it can be seen that both DEM-P, and DEM-C methods gave the results matching the experimental ones in the final part of the plot. In the initial part, the discrepancy between the DEM-C and the experiment can be seen. It can be explained with the fact that in the DEM-C approach the particles are modeled as rigid bodies - what makes the specimen stiffer and causes the slope of the plot steeper. On the other hand - the penalty method captured the physical phenomena of the standard triaxial test at the every stage of the simulation.

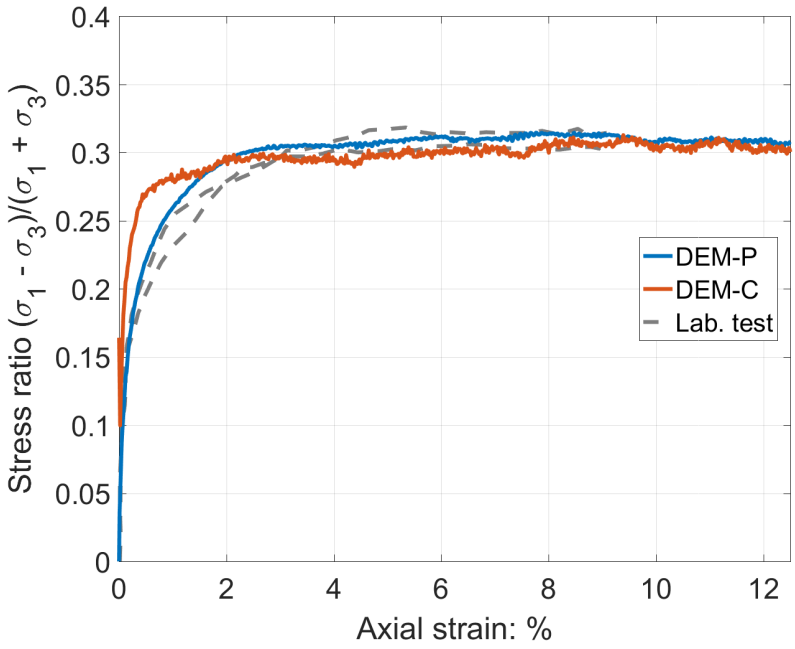

(a) Monodisperse specimen.

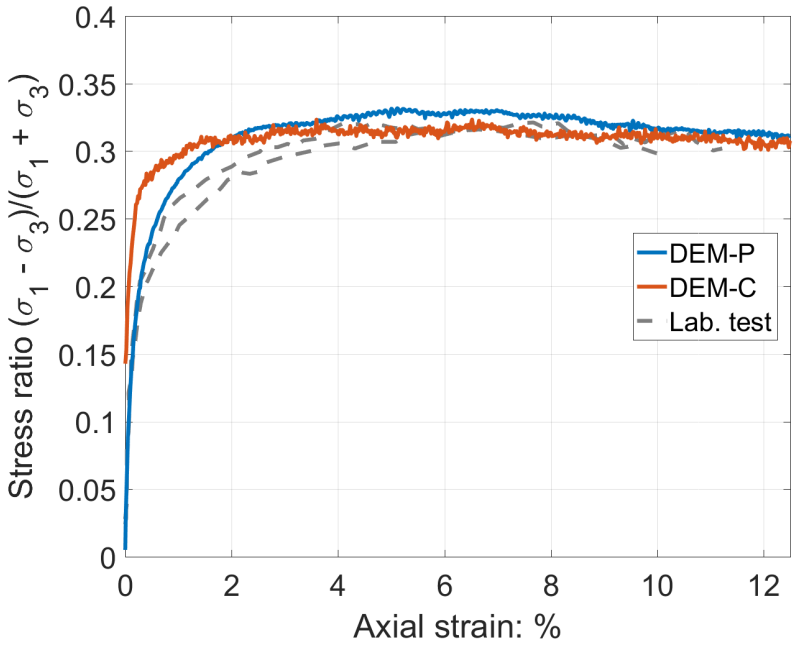

(b) Polydisperse specimen.

Figure 4: Comparison of the experimental and numerical results.

2.4 Performance analysis

To simulate the settling stage and the STT stage using DEM-P approach took in average 1 hour 25 minutes and 4 hours and 55 minutes, respectively (6 hours 20 minutes altogether). The performance of the DEM-C-based simulations was following: 9 hours 21 minutes for the settling and 44 hours and 14 minutes for the STT stage (53 hours 35 minutes altogether). Simulations were run using 10 threads of Intel i5-4300M CPU @ 2.0 GHz.

Table 10: A comparison of the average execution time of the Standard Triaxial Test simulations.

Approach	Stage (Sim. Time. [s])	Exec. Time
DEM-P	Settling (≈ 0.5)	1 h 25 min
	STT (1.5)	4 h 55 min
	Whole (≈ 2.0)	6 h 20 min
DEM-C	Settling (≈ 0.5)	9 h 21 min
	STT (1.5)	44 h 14 min
	Whole (≈ 2.0)	53 h 35 min

3 Additional analyses

3.1 Impact of the $\mu_{\text{particle-side}}$ on the results

The simulation of STT is sensitive to the value of coefficient of friction between the side walls and particles ($\mu_{\text{p-s}}$). The value of the *stress ratio* for larger axial strains

$$f(\sigma_1(\varepsilon, \mu_{\text{p-s}}, \ \ldots), \ \sigma_3) = \frac{\sigma_1 - \sigma_3}{\sigma_1 + \sigma_3} \tag{1}$$

is an increasing function of $\mu_{\text{p-s}}$. In the Fig. 5 curves obtained for $\mu_1^{\text{p-s}} = 0.096$ lay below the ones obtained for $\mu_2^{\text{p-s}} = 0.188$. The values of the other parameters' correspond with those in Tables from 5 to 8. The phenomenon can be easily explained from the physical point of view.

First of all, it has to be noticed that σ_3 does not depend on $\mu_{\text{p-s}}$. This value is dictated by the pressure boundary conditions applied to the side walls. In the simulations conducted on, the pressure on the side walls was equal to the confining pressure applied, $p = 8 \cdot 10^4$ Pa. Hence, $\sigma_3 = p = 8 \cdot 10^4$ Pa in all the simulations.

On the other hand, the value that is explicitly increasing function of $\mu_{\text{p-s}}$ is σ_1 - the pressure the sample acts on the top wall with. There is a displacement boundary condition (actually it is a strain rate BC) applied to the top wall. For larger values of $\mu_{\text{p-s}}$ the mechanical system is less prone to be compressed, thus the sample acts on the top wall with larger pressure.

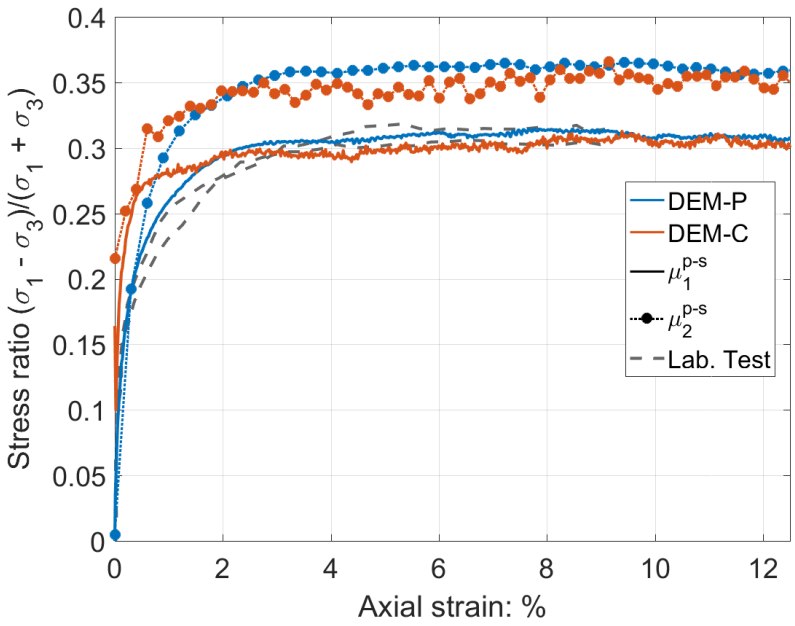

(a) Monodisperse case.

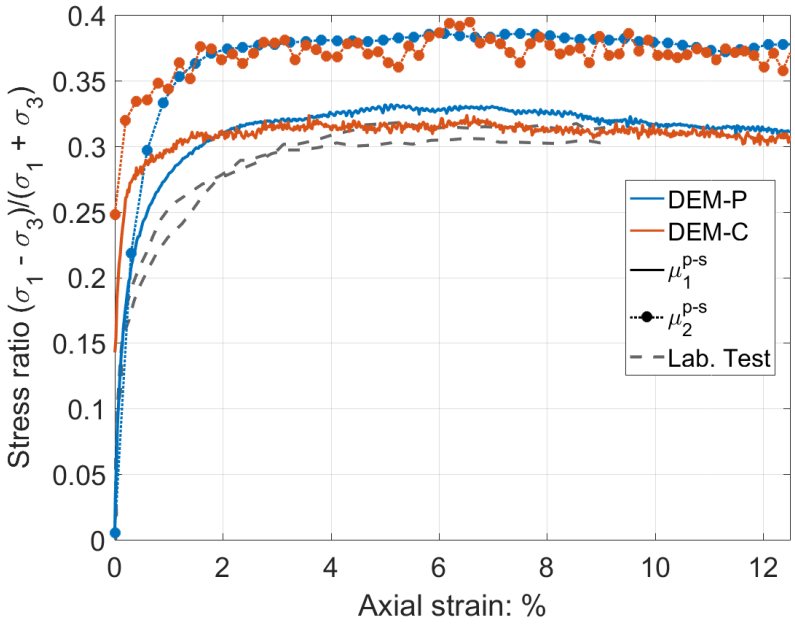

(b) Polydisperse case.

Figure 5: Comparison of the experimental and numerical results.

Table 11: The values of σ_1 and *stress ratio* in the final stage of the standard triaxial test for different values of $\mu_{\text{p-s}}$. Mono. - monodisperse, Poly. - polydisperse specimen; $\sigma_3 = 80$ kPa.

	$\mu_{\text{p-s}}$	σ_1 [kPa]	$(\sigma_1 - \sigma_3)/(\sigma_1 + \sigma_3)$
Mono.	0.096	151	0.307
	0.188	168	0.355
Poly.	0.096	152	0.310
	0.188	176	0.375

The *stress ratio* (1) in an increasing function of σ_1, for the domain of interest ($\sigma_1 \geq \sigma_3$; see equation (2) and Figure 6).

$$f(\sigma_1,\ \sigma_3) = \frac{\sigma_1 - \sigma_3}{\sigma_1 + \sigma_3} = \frac{\sigma_1 + \sigma_3 - 2\sigma_3}{\sigma_1 + \sigma_3} = 1 - \frac{2\sigma_3}{\sigma_1 + \sigma_3},\ \sigma_1 \geq \sigma_3 \tag{2}$$

Since, σ_1 is also an increasing function of $\mu_{\text{p-s}}$, it implies that the *stress ratio* (1) will have larger values for larger $\mu_{\text{p-s}}$.

The values of σ_1 and *stress ratios* for different $\mu_{\text{p-s}}$ were shown in Table. 11. In the Fig. 6 the relation between the *stress ratio* and σ_1 was shown. On the x-axis the values of σ_1 for $\mu_{1,2}^{\text{p-s}}$ were marked. It can be seen that for larger values of $\mu_{\text{p-s}}$, σ_1, as well as $(\sigma_1 - \sigma_3)/(\sigma_1 + \sigma_3)$ have also larger values.

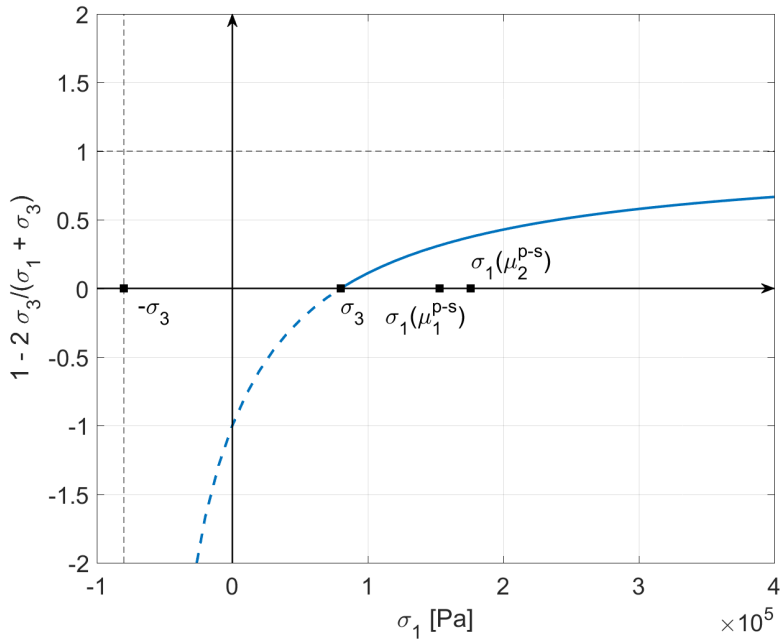

Figure 6: The *stress ratio* as a function of σ_1. On the x-axis the values of σ_1 obtained for $\mu_1^{\text{p-s}} = 0.096$ and $\mu_2^{\text{p-s}} = 0.188$ from the simulations with the polydisperse specimen were marked; $\sigma_3 = 80$ kPa.

3.2 Impact of the MNoI on the results

The simulations of the settling of standard triaxial test using DEM-C approach required up to 700 iterations per time step to make the calculations stable and reasonable from the physical point of view (pressure the specimen acted on the container's walls was equal to the confining pressure applied to the walls). While simulating the second stage - standard triaxial test, more iterations per time step were needed.

For 700 iterations per time step calculations were stable but incorrect from the physical view point. Simulations with maximal number of iterations (MNoI) equal to 1000, 1500, and in case of monodisperse specimen also to 2000, were unstable. Stability and correctness was observed for simulations with MNoI having values higher of equal to 2500 - for monodisperse, and 2000 - for polydisperse specimen (Table 8). The results from simulations with MNoI higher than those threshold values were very similar to each other. It shows that MNoI is a parameter not only responsible for the stability of calculations but it is also important when it comes to modeling the mechanical systems from the physical view point.

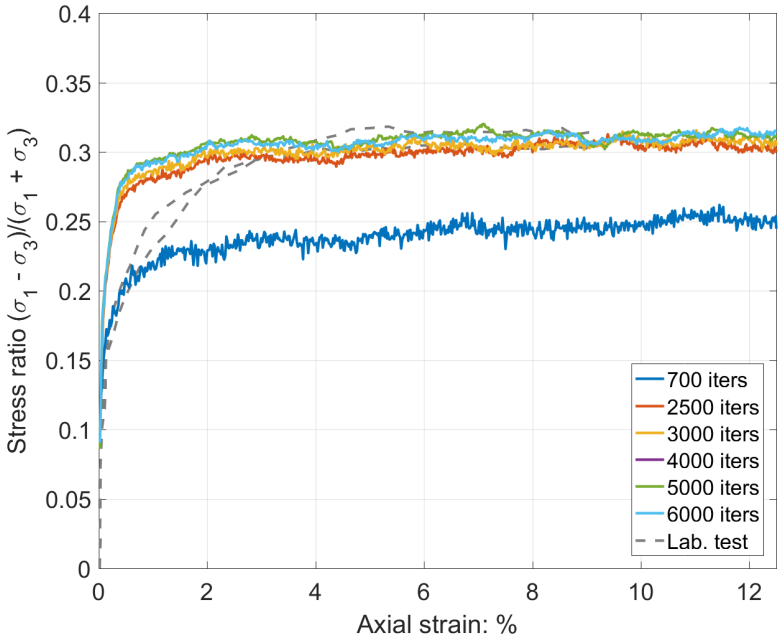

(a)

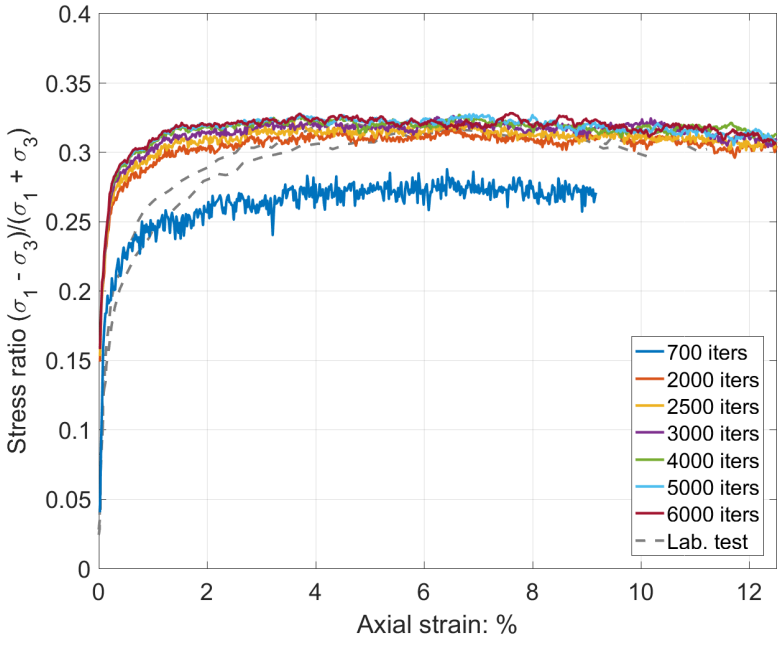

(b)

Figure 7: Comparison of the experimental and numerical results.

4 Conclusion

1. If calibrated properly, both DEM-P and DEM-C approaches can be successfully used in simulating the standard triaxial test.

2. Results obtained from simulations based on those two approaches are comparable.

3. DEM-P-based-simulations were around 10 times faster than the ones based on the DEM-C.

4. In the DEM-C approach the particles are treated as rigid bodies, that is why, for the small values of the axial strain, the slope of the stress-strain curve is steeper than in the reality.

5. The standard triaxial test simulation is sensitive to the value of the coefficient of friction between the particles and side walls.

6. If the simulation is based on the DEM-C approach the number of iterations done during one time step has impact not only on the stability of simulation, but also on the correctness of the results from the physical point of view.

References

[1] Fleischmann, J., 2015. DEM-PM Contact Model with Multi-Step Tangential Contact Displacement History. Tech. Rep. TR-2015-06, Simulation-Based Engineering Laboratory, University of Wisconsin-Madison.

[2] Negrut, D., and Serban, R., 2016. Posing Multibody Dynamics with Friction and Contact as a Differential Algebraic Inclusion Problem. Tech. Rep. TR-2016-12: `http://sbel.wisc.edu/documents/TR-2016-12.pdf`, Simulation-Based Engineering Laboratory, University of Wisconsin-Madison.

[3] ONeill, S., 2005. "A fundamental examination of the behaviour of granular media and its application to discrete element modelling". MsC thesis, University College Dublin, Ireland.

[4] O'Sullivan, C., Bray, J. D., and Riemer, M., 2004. "Examination of the response of regularly packed specimens of spherical particles using physical tests and discrete element simulations". *Journal of Engineering Mechanics-ASCE,* **130**, pp. 1140–1150.

[5] Cui, L., and O'Sullivan, C., 2006. "Exploring the macro- and micro-scale response of an idealised granular material in the direct shear apparatus". *Geotechnique,* **56**, pp. 455–468.

[6] YouTube. Online "Angle of repose movie". `https://www.youtube.com/watch?v=MHTKen1KCAg`. Accessed: 2017-01-07.

[7] Elert, G. The Physics Factbook. Coefficients of Restitution, `http://hypertextbook.com/facts/2006/restitution.shtml`.

[8] Kwarta, M., and Negrut, D., 2016. Using the Complementarity and Penalty Methods for Solving Frictional Contact Problems in Chrono: Validation for the Cone Penetrometer Test. Tech. Rep. TR-2016-16: `http://sbel.wisc.edu/documents/TR-2016-16.pdf`, Simulation-Based Engineering Laboratory, University of Wisconsin-Madison.

[9] Kwarta, M., and Negrut, D., 2016. Using the Complementarity and Penalty Methods for Solving Frictional Contact Problems in Chrono: Validation for the Shear-Test with Particle Image Velocimetry. Tech. Rep. TR-2016-18: `http://sbel.wisc.edu/documents/TR-2016-18.pdf`, Simulation-Based Engineering Laboratory, University of Wisconsin-Madison.

[10] Cui, L., O'Sullivan, C., and O'Neill, S., 2007. "An analysis of the triaxial apparatus using a mixed boundary three-dimensional discrete element model". *Geotechnique,* **57**, pp. 831–844.